High detection sensitivity and reliable morphological correlation of PET with a silicon photomultiplier for primary tongue squamous cell carcinoma

doi: 10.1007/s12149-020-01489-0

Annals of Nuclear Medicine

High detection sensitivity and reliable morphological correlation of PET with a silicon photomultiplier for primary tongue squamous cell carcinoma

--Manuscript Draft--

Manuscript Number:	ANME-D-20-00128R1
Full Title:	High detection sensitivity and reliable morphological correlation of PET with a silicon photomultiplier for primary tongue squamous cell carcinoma
Article Type:	Original article
Corresponding Author:	Ikuho Kojima Tohoku University of Graduate School of Dentistry Sendai, Miyagi JAPAN
Corresponding Author Secondary Information:	
Corresponding Author's Institution:	Tohoku University of Graduate School of Dentistry
Corresponding Author's Secondary Institution:	
First Author:	Ikuho Kojima, DDS, PhD
First Author Secondary Information:	
Order of Authors:	Ikuho Kojima, DDS, PhD
	Kentaro Takanami, MD, PhD
	Takenori Ogawa, MD, PhD
	Maya Sakamoto, DDS, PhD
	Hirokazu Nagai, DDS, PhD
	Hitoshi Miyashita, DDS, PhD
	Masahiro Iikubo, DDS, PhD
Order of Authors Secondary Information:	
Funding Information:	Japan Society for the Promotion of Science London (GB) (18K09804) — Dr. Ikuho Kojima
Abstract:	Objective: A positron emission tomography (PET) scanner using a silicon photomultiplier (SiPM PET) in place of a photomultiplier tube significantly improves the spatial and time resolution. It may also improve the evaluation of smaller lesions compared to conventional (non-SiPM) PET scanners. We compared the maximum standardized uptake value (SUVmax), detection sensitivity, and morphological correlation using magnetic resonance imaging (MRI) for primary tongue squamous cell carcinoma between the SiPM PET and non-SiPM PET scanner. Methods: We retrospectively reviewed the F-18 fluorodeoxyglucose (FDG) PET/CT features of tongue squamous cell carcinomas in consecutive, newly diagnosed, and pathologically verified patients. Twenty-five of 46 patients were scanned using SiPM PET scanner and the remaining 21 patients were scanned with a non-SiPM PET scanner. We compared the SUVmax and visual evaluation of primary tumor detectability, and the correlation between the PET-based and MRI-based tumor size (long axis, thickness, and volume). Differences in SUVmax and detection sensitivity for the primary tumor were analyzed using Welch's t -test and Fisher's exact test, respectively. Correlations among the PET-based, MRI-based tumor size, and SUVmax were assessed using Spearman's rank correlation coefficient. Results: SUVmax of both T1/T2 and T3/T4 primary tumors were significantly higher for the SiPM PET (T1/T2 mean SUVmax: 6.6 ± 4.3, T3/T4 mean SUVmax: 18.2 ± 9.8) than that for the non-SiPM PET (T1/T2 mean SUVmax: 3.4 ± 1.4, T3/T4 mean SUVmax: 10.2 ± 4.9) ($P < 0.05$). While all cases of T3/T4 primary tumors were

	detected by both PET scanners, the detection sensitivity for T1/T2 primary tumors was significantly higher for the SiPM PET (80%) than that for the non-SiPM PET (36.4%) ($P < 0.05$). MRI-based tumor size correlated significantly with SiPM PET-based tumor long axis ($\rho = 0.74$) and volume ($\rho = 0.91$), but not with the non-SiPM PET-based tumor long axis and volume in T1/T2 primary lesions. Correlation between MRI-based tumor size and SUVmax was significant in both PET scanners; however, no significant difference was observed between the two scanners. Conclusions : The SiPM PET provides better detection sensitivity and a reliable morphological correlation for the T1/T2 primary tongue tumors than the non-SiPM PET due to its high performance.
Author Comments:	

Original Research–Head and Neck

High detection sensitivity and reliable morphological correlation of PET with a silicon photomultiplier for primary tongue squamous cell carcinoma

Ikuho Kojima, DDS, PhD[1,4], Kentaro Takanami, MD, PhD[2], Takenori Ogawa MD, PhD[3,4], Maya Sakamoto DDS, PhD[1,4], Hirokazu Nagai DDS, PhD[4,5], Hitoshi Miyashita DDS, PhD[4,5], Masahiro Iikubo DDS, PhD[1,4]

Short title: Semiconductor PET of tongue cancer

[1]Department of Oral Diagnosis, Tohoku University Graduate School of Dentistry, 4-1 Seiryo-machi, Aoba-ku, Sendai, Miyagi 980-8575, Japan

[2]Department of Diagnostic Radiology, Tohoku University Hospital, 1-1 Seiryo-machi, Aoba-ku, Sendai, Miyagi 980-8574, Japan

[3]Department of Otolaryngology-Head and Neck Surgery, Tohoku University Hospital, 1-1 Seiryo-machi, Aoba-ku, Sendai, Miyagi 980-8574, Japan

[4]Head and Neck Cancer Center, Tohoku University Hospital, 1-1 Seiryo-machi, Aoba-

ku, Sendai, Miyagi 980-8574, Japan

[5]Department of Oral and Maxillofacial Surgery, Tohoku University Graduate School of Dentistry, 4-1 Seiryo-machi, Aoba-ku, Sendai, Miyagi 980-8575, Japan

Corresponding author:

Ikuho Kojima

Department of Oral Diagnosis, Tohoku University Graduate School of Dentistry

4-1 Seiryo-machi, Aoba-ku, Sendai, Miyagi 980-8575, Japan

Tel: 81-22-717-8390

Fax: 81-22-717-8393

E-mail: ikh-koji213@dent.tohoku.ac.jp

Type of article: Original article

Funding

This study was supported by Japan Society for the Promotion of Science (JSPS) Grants-in-Aid for Scientific Research (Grant Number 18K09804).

Semiconductor PET of tongue cancer

Abstract

Objective: A positron emission tomography (PET) scanner using a silicon photomultiplier (SiPM PET) in place of a photomultiplier tube significantly improves the spatial and time resolution. It may also improve the evaluation of smaller lesions compared to conventional (non-SiPM) PET scanners. We compared the maximum standardized uptake value (SUVmax), detection sensitivity, and morphological correlation using magnetic resonance imaging (MRI) for primary tongue squamous cell carcinoma between the SiPM PET and non-SiPM PET scanner.

Methods: We retrospectively reviewed the F-18 fluorodeoxyglucose (FDG) PET/CT features of tongue squamous cell carcinomas in consecutive, newly diagnosed, and pathologically verified patients. Twenty-five of 46 patients were scanned using SiPM PET scanner and the remaining 21 patients were scanned with a non-SiPM PET scanner. We compared the SUVmax and visual evaluation of primary tumor detectability, and the correlation between the PET-based and MRI-based tumor size (long axis, thickness, and volume). Differences in SUVmax and detection sensitivity for the primary tumor were analyzed using Welch's *t*-test and Fisher's exact test, respectively. Correlations among the PET-based, MRI-based tumor size, and SUVmax were assessed using Spearman's rank correlation coefficient.

Results: SUVmax of both T1/T2 and T3/T4 primary tumors were significantly higher for the SiPM PET (T1/T2 mean SUVmax: 6.6 ± 4.3, T3/T4 mean SUVmax: 18.2 ± 9.8) than that for the non-SiPM PET (T1/T2 mean SUVmax: 3.4 ± 1.4, T3/T4 mean SUVmax: 10.2 ± 4.9) ($P < 0.05$). While all cases of T3/T4 primary tumors were detected by both PET scanners, the detection sensitivity for T1/T2 primary tumors was significantly higher for the SiPM PET (80%) than that for the non-SiPM PET (36.4%) ($P < 0.05$). MRI-based tumor size correlated significantly with SiPM PET-based tumor long axis ($\rho = 0.74$) and volume ($\rho = 0.91$), but not with the non-SiPM PET-based tumor long axis and volume in T1/T2 primary lesions. Correlation between MRI-based tumor size and SUVmax was significant in both PET scanners; however, no significant difference was observed between the two scanners.

Conclusions: The SiPM PET provides better detection sensitivity and a reliable morphological correlation for the T1/T2 primary tongue tumors than the non-SiPM PET due to its high performance.

Keywords: F-18 fluorodeoxyglucose PET/CT (F-18 FDG PET/CT), silicon photomultiplier, tongue cancer

Introduction

In diagnostic imaging of primary malignant tumors, computed tomography (CT) and magnetic resonance imaging (MRI) are highly useful modalities for evaluating the size and extension of lesions. The evaluation of primary oral tumors on CT is often useless due to dental metal artifacts, and that on MRI is also sometimes difficult. F-18 fluorodeoxyglucose (FDG) positron emission tomography/computed tomography (PET/CT) for primary lesions is particularly important for evaluating the tumor metabolic activity, determining the presence or absence of local recurrence after surgery, assessing the treatment effects of chemoradiotherapy, and prognosis prediction [1-5]. In oral cancer, interstitial brachytherapy is sometimes applied for T1-2 lesions, and superselective intra-arterial chemoradiotherapy is increasingly applied for advanced tumors as a definite treatment [6-8]. Therefore, it is important to evaluate the metabolic activity and tumor size on PET in order to determine the prognostic prediction, treatment effect, and presence or absence of local recurrence. In particular, it is essential to accurately evaluate the tumor activity and morphology on PET, even for a superficial and small lesion in case of the small recurrent tumor, tumor regressed by treatment, T1-2 lesion, or useless on CT or MRI due to metal artifact.

However, the FDG accumulation level is underestimated due to the partial-

volume effect when the tumor is small; this is considered a disadvantage of the PET examination [9, 10]. The partial-volume effect typically occurs whenever a tumor size is less than approximately three times the spatial resolution, and smaller lesions are therefore evaluated as having a smaller standardized uptake value (SUV) [9]. The recovery coefficient (RC) for a 10 mm-diameter hot sphere ($RC_{10\ mm}$) filled with a radioisotope (RI) solution of our conventional PET/CT scanner, which is in use at our hospital, is 41%. That is, for lesions of 10 mm uptake size, the SUV is theoretically 41% of the true value. Primary tumors with small and superficial lesions are likely to be underestimated by PET. Thus, PET-based quantitative analysis of T1/T2 oral primary tumors, whose thickness is less than 10 mm, is not likely to be accurate. Therefore, many oral cancers go undetected and the maximum SUV (SUVmax) and size of the tumor is underestimated.

A PET scanner using a silicon photomultiplier (SiPM) instead of a photomultiplier tube has recently been developed. Many technological improvements of this new PET system have been made, in terms of both hardware and software, resulting in better imaging quality, higher spatial resolution, and more accurate image reconstruction [11, 12]. The $RC_{10\ mm}$ of the PET scanner using the SiPM at our hospital is 71%, which is far superior to the $RC_{10\ mm}$ of a conventional PET (41%). On the other hand,

the RC for > 20-mm-diameter hot sphere of a RI is almost 100% for both the SiPM and conventional PET scanners. Therefore, the PET scanner using SiPM with improved quantitative ability for small objects can be expected to be more sensitive than the conventional PET scanners for the detection of small lesions [13]. Moreover, the SiPM PET should be able to accurately evaluate the tumor activity and morphology, such as the tumor length, thickness, and volume for primary oral tumors as most of them are small/superficial tumors such as the T1/T2 lesions. Herein, we compared the detection sensitivity, SUVmax, and the correlation between PET-based and MRI-based morphological size of the primary tongue tumors determined by the PET scanner using SiPM (SiPM PET) and by a conventional PET scanner (non-SiPM PET).

Materials and methods

We performed this study in accordance with the Declaration of Helsinki. Informed consent was obtained from all individual participants included in the study. The relevant institutional review board approved this retrospective study (No. 2017-3-34).

Patients

We retrospectively reviewed 49 consecutive patients, newly diagnosed with a tongue squamous cell carcinoma. They all underwent F-18 FDG-PET/CT, ultrasonography (USG), and contrast-enhanced MRI for cancer staging before treatment, between October 2016 and January 2019. These cases were all confirmed by pathological diagnosis. We excluded three of 49 patients because of a biopsy performed within a week before these imaging examinations and enrolled the remaining 46 patients in this study (26 men, 20 women; age range, 21–94 years; mean age, 65.9 years). We investigated the primary tumor classification, diameter, thickness, and histopathological grade to evaluate bias between the cases scanned with SiPM and non-SiPM PET. The clinical T category (cT) was determined according to the eighth edition of the TNM classification of malignant tumors edited by the Union for International Cancer Control [14]. We defined the tumor diameter as the maximum size in the axial or coronal plane

on an MRI. We prioritized the USG measurements in tumor thickness for determining the cT stage. We investigated the histopathological grade of the mode of invasion by using the modified Jakobsson criteria [15, 16], and the degree of differentiation using the WHO classification of tumor malignancy gradation [17]. Pathological tumor size (tumor long axis and tumor thickness from the tongue surface) was investigated except for the 16 cases in which the measurements could not be performed pathologically.

Imaging technique

Twenty-five of 46 patients were imaged using a SiPM PET/CT scanner (Discovery MI, GE Healthcare, Fairfield, US), and the remaining 21 patients by a conventional PET/CT scanner (TruePoint Biograph 40, Siemens Medical Solutions, Erlangen, Germany). The SiPM or non-SiPM PET examination was randomly selected for each patient. After a 4-hour fast, the patients were injected with 3.7 MBq (0.1 mCi) F-18 FDG/kg body weight. All patients required a blood glucose level of < 200 mg/dl before the FDG injection. One hour after the injection, a spiral CT scan was performed using 60–100 mAs (automatic exposure control), 120 kVp, and 3.75-mm slice thickness in the SiPM PET/CT scanner, or 25 effective mAs, 130 kVp, and 5-mm slice thickness in the non-SiPM PET/CT scanner, followed by a PET scan from the distal femur to the top of the

skull. A SiPM PET scan was performed using a 2-min scanning time per bed position, increments of 19.5 cm (3D mode), and seven bed-positions. A non-SiPM PET scan was performed using a 2-min scanning time per bed position, increments of 16.2 cm (3D mode), and eight bed-positions. The SiPM PET images were reconstructed using the newly developed algorithms (block sequential regularized expectation maximization, β = 600) to a final pixel size of 3.6 mm × 3.6 mm × 2.7 mm. The non-SiPM PET images were reconstructed using the iterative algorithms (ordered-subset expectation maximization, four iterations, and 21 subsets) to a final pixel size of 4.1 mm × 4.1 mm × 2.0 mm. An 8-mm full-width at half-maximum Gaussian filter was applied after the reconstruction.

MRI examinations were performed using a 1.5T MR imager (Achieva 1.5T Nova Dual, Philips Medical Systems, Eindhoven, Netherlands) or a 3.0T MR imager (Achieva 3.0T dStream or Ingenia 3.0T CX, Philips Medical Systems, Eindhoven, Netherlands) with the head and neck coil. MRI protocols are as follows: transverse fat-suppressed T2-weighted images (3500–5000/49–90 [repetition time msec/echo time msec], field of view 230–250 mm, acquisition matrix 256 × 256, 320 × 320, 400 × 400, and section thickness 5 mm), transverse fat-suppressed postcontrast T1-weighted images (538–783/8–10, field of view 230–250 mm, acquisition matrix 320 × 320, 504 ×

504, 548 × 548, and section thickness 5–7 mm) with an intravenous infusion of 0.2 ml/kg body weight gadolinium contrast agents (Magnescope, meglumine gadoterate, Guerbet Japan, Tokyo, Japan; Gadovist, Gadobutrol, Bayer HealthCare, Berlin, Germany).

Image analysis

Board-certified oral and maxillofacial radiologists (MI and MS, with 24 and 36 years of experience, respectively) independently reviewed the randomly ordered PET images, while being blinded to all clinical information other than that the PET images were obtained from patients with a tongue tumor. The reviewers visually evaluated the presence or absence of an abnormal FDG accumulation suspected of representing the primary tongue tumor, both on pre- and post-attenuation corrected PET images. Reviewers resolved disagreements in assessment by discussion. Another board-certified oral and maxillofacial radiologist (IK with 16 years of experience), who knew the site of the primary tumors, reviewed the randomly ordered PET images and measured the SUVmax, morphological tumor size: long axis (the length in the transverse plane), thickness (depth from tongue surface in the transverse plane), and the volume of the primary tumor while taking care to avoid the high physiological accumulation areas

other than the tumor. The reviewer also reviewed the randomly ordered MRI and measured the same morphological tumor sizes (long axis, thickness, and volume) on the transverse fat-suppressed T2-weighted images or transverse fat-suppressed postcontrast T1-weighted images. The measurements of tumor volume were calculated as the sum of all transverse section areas, multiplied by the section thickness, as previously reported [18].

Statistical analysis

Detection sensitivity for the primary tumor, sex ratio, and T category ratio was compared between the groups, examined by SiPM PET or non-SiPM PET scanner, by using the Fisher's exact test. Welch's *t*-test was used to analyze the differences in the SUVmax and mean age of patients between the two groups. The Mann–Whitney U-test was used to analyze the differences in the histological grade (mode of invasion and degree of differentiation) and tumor morphology (major axis, thickness, and volume) between the two groups. Correlations among the PET-based, MRI-based, pathological tumor sizes, and SUVmax were tested by Spearman's rank correlation coefficient (ρ). The strength of correlation was classified as negligible or no correlation ($|\rho| \leq 0.20$), weak ($|\rho| = 0.21$ to 0.40), moderate ($|\rho| = 0.41$ to 0.70), or strong ($|\rho| = 0.71$ to 1.00). All

p-values were two-sided and p-values of < 0.05 were considered statistically significant. For statistical analysis, we used the EZR software (Saitama Medical Center, Jichi Medical University), which provides a graphical interface for R (version 3.2.2; The R Foundation for Statistical Computing, Vienna, Austria).

Results

Characteristics of patients and primary tumors

The mean age of the patients examined by SiPM PET was 66.1 ± 19.4 years, and that of those examined by non-SiPM PET was 65.6 ± 10 years. Of the 25 primary tumors examined by SiPM PET, six were clinically diagnosed as being T1 tumors, nine were T2 tumors, six were T3 tumors, and four were T4 tumors. Of the 21 primary tumors examined by non-SiPM PET, three were clinically diagnosed as T1 tumors, eight were T2 tumors, five were T3 tumors, and five were T4 tumors. No tumor was histopathologically upgraded in the clinical T category of the TNM classification. There were no significant differences in the primary tumor volume, major axis, thickness, the histopathological grade of the mode of invasion, and the degree of differentiation between the patients examined by the two types of PET scanners. No significant differences were found between the two groups in other histological parameters, i.e., microvascular invasion, perineural invasion, and lymphatic vascular invasion (data not shown). Detailed clinical profiles of the patients and primary tumors are shown in Table 1.

FDG-PET/CT features

Many cases of T1/T2 primary tumors were detectable by the SiPM PET but not by the non-SiPM PET (**Figure 1**). All cases of T3/T4 primary tumors were detectable by both the SiPM PET and non-SiPM PET (**Figure 2**). The detection sensitivity for T1/T2 primary tumors was 80% by SiPM PET and 36.4% by non-SiPM PET. The detection sensitivity for T1/T2 primary tumors was therefore significantly higher with the SiPM PET than that with the non-SiPM PET ($P < 0.05$) (**Figure 3a**). For T3/T4 primary tumors, detection sensitivity was 100% by both the PET scanners (**Figure 3b**). The SUVmax of the T1/T2 primary tumors was 6.6 ± 4.3 in the SiPM PET and 3.4 ± 1.4 in the non-SiPM PET groups. Thus, the SUVmax of the T1/T2 primary tumors was significantly higher in the SiPM PET than that in the non-SiPM PET group ($P < 0.05$) (**Figure 3c**). The SUVmax of the T3/T4 primary tumors was 18.2 ± 9.8 in the SiPM PET and 10.2 ± 4.9 in the non-SiPM PET group. Thus, the SUVmax of the T3/T4 primary tumors was also significantly higher in the SiPM PET than that in the non-SiPM PET group ($P < 0.05$) (**Figure 3d**).

Correlation between PET and other parameters

The pathological tumor size was significantly correlated with the MRI-based ($\rho = 0.74$ and 0.88) and the SiPM PET-based ($\rho = 0.65$ and 0.81) tumor size (long axis and

thickness, respectively), and the non-SiPM PET-based tumor thickness (ρ = 0.69), but not with the non-SiPM PET-based long axis (**Figure 4a-f**). These ρ values between the pathological and MRI-based long axis and thickness, and between the pathological and SiPM PET-based thickness, exhibited a strong correlation.

MRI-based tumor long axis and volume were significantly correlated with the SiPM PET-based long axis and volume (long axis: ρ = 0.74, volume: ρ = 0.91), but not with the non-SiPM PET-based tumor long axis and volume in the T1/T2 primary lesions (**Figure 5a, 5b, 5e, and 5f**). Both ρ values exhibited a strong correlation. MRI-based tumor thickness was not correlated with both the SiPM and non-SiPM PET-based thickness in the T1/T2 primary lesions (**Figure 5c and 5d**). In T3/T4 lesions, MRI-based tumor size (long axis, thickness, and volume) were all significantly correlated with both the SiPM PET-based (long axis: ρ = 0.65, thickness: ρ = 0.80, volume: ρ = 0.95) and the non-SiPM PET-based (long axis: ρ = 0.68, thickness: ρ = 0.77, volume: ρ = 0.97) tumor size (data not shown).

MRI-based tumor sizes (long axis, thickness, and volume) were all significantly correlated with the SUVmax in both the SiPM (long axis: ρ = 0.73, thickness: ρ = 0.76, volume: ρ = 0.77) and non-SiPM PET (long axis: ρ = 0.55, thickness: ρ = 0.75, volume: ρ = 0.76) (**Figure 6a-f**). These ρ values exhibited a strong

correlation except for a moderate correlation between the MRI-based long axis and SUVmax in non-SiPM PET.

Discussion

In this study, we analyzed the detection sensitivity for primary tongue tumors of a SiPM PET scanner in comparison with the conventional non-SiPM PET scanner. The SiPM PET scanner demonstrated better imaging quality, higher spatial resolution, and more accurate imaging reconstruction than the conventional PET scanner. The detection sensitivity for T1/T2 primary tumors was significantly higher for the SiPM PET than that for the non-SiPM PET scanner, while both types of scanners could detect the T3/T4 primary tumors. The SUVmax for all T-stages of primary tumors was significantly higher for the SiPM PET than that for the non-SiPM PET scanner, and the SiPM PET-based tumor size had a stronger significant correlation with the pathological and MRI-based tumor size than the non-SiPM PET-based tumor size.

The SUVmax of T1/T2 tumors in the SiPM PET was about twice of that in the non-SiPM PET (**Figure 3c**). The difference in the SUVmax suggests that non-SiPM PET underestimates the quantification of primary tumors, whereas the SiPM PET performs a more accurate quantitative evaluation. Differences in the scanner performance in terms of radiation sensitivity, spatial resolution, and imaging reconstruction influence the SUV quantitative ability. Roncali et al. [11] reported that the PET scanner using SiPM has significantly improved radiation sensitivity, spatial

resolution, and imaging reconstruction. Teo et al. [10] reported that SiPM PET had improved SUV quantitative ability for small objects, both in phantoms and the patients. In patients who had undergone both the SiPM PET and non-SiPM PET examinations, SUVmax of the various accumulations, such as physiological and pathological accumulation, was higher in the SiPM PET than that in the non-SiPM PET [13]. Baratto et al. [13] compared the SUVmax of various lesions between the SiPM and non-SiPM PET and found that the SUVmax was higher for the SiPM PET. The $RC_{10\ mm}$, which is affected by the spatial resolution, was 71% in our SiPM PET scanner, which was far superior to the $RC_{10\ mm}$ of 41% of our hospital's non-SiPM PET scanner. Thus, in accordance with the previous reports, our study demonstrated that the high SUVmax of primary T1/T2 tongue tumors is likely to exhibit a more accurate quantitative ability of SiPM PET due to the high performance of the scanner in terms of spatial resolution. On the other hand, the SUVmax of T3/T4 tumors was also significantly higher in the SiPM PET than that in the non-SiPM PET (**Figure 3d**). Since the RC for > 20-mm-diameter hot sphere of an RI is almost 100% for both the SiPM and non-SiPM PET scanners, it is reasonable to consider that the difference of metabolic activity is highly likely to significantly influence the SUVmax of the T3/T4 tumors rather than the difference of the scanner's performance. The expression of the glucose transporters, Glut1 and Glut4,

which are key regulators of F-18 FDG, highly influence the SUVmax. We should have analyzed the expression of the Glut1 and Glut4 using immunohistology or quantitative PCR but were unable to perform such analyses in our retrospective study. Thus, the biological aspect is a major limitation of this study. Furthermore, we should design a prospective study that performs consecutive SiPM and non-SiPM PET for the same lesion to avoid the tumor metabolic differences in a future study.

The detection sensitivity for T1/T2 primary tongue tumors by the SiPM PET was more than two-fold than that of the non-SiPM PET. We demonstrated that SiPM PET was significantly better than the non-SiPM PET for the detection of T1/T2 primary tongue tumors (**Figure 3a**). The detection sensitivity for T3/T4 primary tumors was 100% for both the PET scanners (**Figure 3b**). These results showed that the SiPM PET had a higher detection sensitivity than the non-SiPM PET for smaller tongue tumors. Yamazaki et al. [19] reported that FDG-PET exhibited a 100% detection sensitivity for metastatic lymph nodes that had a short-axis diameter of more than 10 mm, but did not detect those smaller than 5 mm. Our study demonstrated an improved sensitivity of SiPM PET for detecting primary tumors that are less than 5 mm thickness, which has not been directly shown in previous studies.

The significant correlation between the pathological and SiPM PET-based

tumor thickness (ρ = 0.81) was stronger than that between the pathological and non-SiPM PET-based thickness (ρ = 0.69) (**Figure 4d and 4f**). The pathological long axis significantly correlated with the SiPM PET-based long axis (ρ = 0.65), but not with the non-SiPM PET-based long axis (**Figure 4c and 4e**). Moreover, MRI-based tumor size, which had an extremely strong correlation with the pathological tumor size (long axis: ρ = 0.74, thickness: ρ = 0.88) (**Figure 4a and 4b**), was significantly correlated with the SiPM PET-based tumor size (long axis: ρ = 0.74, volume: ρ = 0.91) but not with non-SiPM PET-based tumor long axis and volume in the T1/T2 primary lesions (**Figure 5a, 5b, 5e, and 5f**). Yu et al. [20] reported that the tumor size (X-, Y-, Z-axis) measured on FDG PET/CT correlated more reliably with the pathological findings than that on a CT. Koopman et al. [21] and Nguyen et al. [22] prospectively evaluated the performance of a SiPM PET in patients with various cancer compared to a non-SiPM PET and demonstrated that the SiPM PET-based tumor volume significantly decreased by 13-30%, compared to the non-SiPM PET. They suggest that these decreases in tumor volume were likely caused by the higher resolution of the SiPM PET system that decreases the partial-volume effect. Similar to these three studies, our result showed that the non-SiPM PET-based tumor size tended to increase in the T3/T4 lesions (data not shown). Moreover, non-SiPM PET-based volume decreased due to the underestimation

of the FDG uptake and did not correlate with the MRI-based tumor volume in the T1/T2 lesions (**Figure 5f**). In contrast, SiPM PET strongly correlated with the MRI-based tumor volume, even small and superficial tumors. These results were largely due to the high performance of the SiPM PET scanner. Thus, SiPM PET had a more reliable morphological correlation for T1/T2 primary tongue tumors than the non-SiPM PET. The tumor volume used for treatment effect and prognosis prediction had a particularly high correlation between the SiPM PET-based and MRI-based volume ($\rho = 0.91$) and SiPM PET may be useful for the evaluation in those treatment planning based on both the metabolic and morphological aspects.

MRI-based tumor size (long axis, thickness, and volume) were all significantly correlated with the SUVmax in both the SiPM (long axis: $\rho = 0.73$, thickness: $\rho = 0.76$, volume: $\rho = 0.77$) and non-SiPM PET (long axis: $\rho = 0.55$, thickness: $\rho = 0.75$, volume: $\rho = 0.76$) (**Figure 6a-f**). These results were similar to the linear proportional relationship between the RC and the sphere diameter [10] and demonstrated that the SUVmax tended to increase with the tumor size (long axis, thickness, and volume) in the tongue primary tumor. However, unlike the RC measured by a phantom, tumor SUVs exhibited different values depending on their biological activity. Therefore, this correlation data may be the result of confusion between the scanner performance and

biological activity. No significant difference may exist in the correlation coefficient between the two scanners due to the influence of the biological activity, similar to the limitation mentioned before.

As a limitation of this study and as a consideration for future research, the effects of metal artifacts on PET images were not taken into account in this study. In general, X-ray attenuation correction based on CT is difficult when metal artifacts occur. It has been pointed out that CT-based attenuation correction results in overestimation of tracer accumulation in the areas corresponding to bright streak artifacts on CT images [23-25]. Shimamoto et al. [25] also reported that underestimation might occur due to a decrease in radiation sensitivity when the tumor was in contact with a dental metal prostheses. We were able to prevent the overestimation of the tracer accumulation entirely by inspecting both attenuation correction and non-attenuation correction PET images in our research, as recommended by Shimamoto et al. [25]. On the other hand, underestimation of the lesions around dental metal prostheses should be taken into consideration. In our study, because there was no bias in the amount of metal artifact between the two groups and the availability of tumor detection, the metal artifacts had little impact on our results. However, it may be necessary to conduct a more detailed investigation using a phantom to ascertain the effects of metal artifacts.

Additionally, it will be necessary to examine other oral cancers with a more complicated anatomy, which cannot be expressed in a simple manner in terms of diameter in the oral cavity. In future, the goal is to apply this high-resolution PET scanner to the evaluation of tumor activity and prognosis prediction, and thereby contribute to treatment decision.

Another major limitation of this study is that we did not consider the motion artifact of the tongue. In an MRI study, where the scan times were similar to that of PET, Suzuki et al. [26] investigated the influence of the motion artifact on tongue morphological size. They concluded that wearing dentures during an MRI examination reduces the motion artifacts in edentulous patients without any occlusal support. Although we could not analyze the presence or absence of the occlusal support in the patients of the present study, we believe that motion artifacts are greatly related to individual differences other than occlusal support. On the other hand, although the tumors shrink during the surgical excision and fixation in buffered formalin, MRI-based tumor size has demonstrated a marked correlation with the histopathological thickness in several reports [27-31]. Since MRI and PET may, on occasion, over-estimate the tumor size in cases of recent biopsy and inflammation, we excluded the three patients who had undergone biopsy within a week before these imaging examinations. As a result, the correlation between the pathological and MRI-based tumor size was

extremely strong. The correlation between the MRI-based and PET-based tumor size was also strong in the present study. Consequently, although the influence of motion artifacts cannot be ruled out, the morphological measurement and correlation of the tongue tumor are likely to be highly reliable.

Conclusion

The SiPM PET demonstrated superior detection sensitivity and more reliable morphological correlation for the T1/T2 primary tongue tumors than the non-SiPM PET, due to the high performance of the scanner.

References

1. Kunkel M, Forster GJ, Reichert TE, Jeong JH, Benz P, Bartenstein P, et al. Detection of recurrent oral squamous cell carcinoma by [18F]-2-fluorodeoxyglucose-positron emission tomography: implications for prognosis and patient management. Cancer 2003;98(10):2257-65.

2. Rege S, Safa AA, Chaiken L, Hoh C, Juillard G, Withers HR. Positron emission tomography: an independent indicator of radiocurability in head and neck carcinomas. Am J Clin Oncol 2000;23(2):164-9.

3. Dibble EH, Alvarez AC, Truong MT, Mercier G, Cook EF, Subramaniam RM. 18F-FDG metabolic tumor volume and total glycolytic activity of oral cavity and oropharyngeal squamous cell cancer: adding value to clinical staging. J Nucl Med 2012;53(5):709-15.

4. Avril NE, Weber WA. Monitoring response to treatment in patients utilizing PET. Radiol Clin North Am 2005;43(1):189-204.

5. Doi H, Kitajima K, Fukushima K, Kawanaka Y, Mouri M, Yamamoto S, et al. SUVmax on FDG-PET is a predictor of prognosis in patients with maxillary sinus cancer. Jpn J Radiol 2016;34(5):349-55.

6. Oyama T, Hosokawa Y, Abe K, Hasegawa K, Fukui R, Aoki M, et al.

Prognostic value of quantitative FDG-PET in the prediction of survival and local recurrence for patients with advanced oral cancer treated with superselective intra-arterial chemoradiotherapy. Oncol Lett. 2020;19(6): 3775–80.

7. Shimizu M, Mitsudo K, Koike I, Taguri M, Iwai T, Koizumi T, et al. Prognostic value of 2-[(18) F]fluoro-2-deoxy-D-glucose positron emission tomography for patients with oral squamous cell carcinoma treated with retrograde superselective intra-arterial chemotherapy and daily concurrent radiotherapy. Oral Surg Oral Med Oral Pathol Oral Radiol 2016;121(3):239-47.

8. Leung TW, Wong VY, Kwan KH, Ng TY, Wong CM, Tung SY et al. High dose rate brachytherapy for early stage oral tongue cancer. Head Neck 2002;24(3):274-81.

9. Soret M, Bacharach SL, Buvat I. Partial-volume effect in PET tumor imaging. J Nucl Med 2007;48(6):932-45.

10. Teo BK, Seo Y, Bacharach SL, Carrasquillo JA, Libutti SK, Shukla H, et al. Partial-volume correction in PET: validation of an iterative postreconstruction method with phantom and patient data. J Nucl Med 2007;48(5):802-10.

11. Roncali E, Cherry SR. Application of silicon photomultipliers to positron emission tomography. Ann Biomed Eng 2011;39(4):1358-77.

12. Teoh EJ, McGowan DR, Macpherson RE, Bradley KM, Gleeson FV. Phantom

and Clinical Evaluation of the Bayesian Penalized Likelihood Reconstruction Algorithm Q.Clear on an LYSO PET/CT System. J Nucl Med 2015;56(9):1447-52.

13. Baratto L, Park SY, Hatami N, Davidzon G, Srinivas S, Gambhir SS, et al. 18F-FDG silicon photomultiplier PET/CT: A pilot study comparing semi-quantitative measurements with standard PET/CT. PLoS One 2017;12(6):e0178936.

14. Brierley J, Gospodarowicz MK, Wittekind C. TNM classification of malignant tumours. Eighth edition. ed. Chichester, West Sussex, UK ; Hoboken, NJ: John Wiley & Sons, Inc.; 2017;p.17-21.

15. Jakobsson PA, Eneroth CM, Killander D, Moberger G, Martensson B. Histologic classification and grading of malignancy in carcinoma of the larynx. Acta Radiol Ther Phys Biol 1973;12(1):1-8.

16. Yamamoto E, Kohama G, Sunakawa H, Iwai M, Hiratsuka H. Mode of invasion, bleomycin sensitivity, and clinical course in squamous cell carcinoma of the oral cavity. Cancer 1983;51(12):2175-80.

17. Pindborg JJ. Reichart PA, Smith CJ, van der Waal I. Histological Typing of Cancer and Precancer of the Oral Mucosa. WHO; 1997.

18. Kojima I, Sakamoto M, Iikubo M, Kumamoto H, Muroi A, Sugawara Y, et al. Diagnostic performance of MR imaging of three major salivary glands for Sjogren's

syndrome. Oral Dis 2017;23(1):84-90.

19. Yamazaki Y, Saitoh M, Notani K, Tei K, Totsuka Y, Takinami S, et al. Assessment of cervical lymph node metastases using FDG-PET in patients with head and neck cancer. Ann Nucl Med 2008;22(3):177-84.

20. Yu HM, Liu YF, Hou M, Liu J, Li XN, Yu JM. Evaluation of gross tumor size using CT, 18F-FDG PET, integrated 18F-FDG PET/CT and pathological analysis in non-small cell lung cancer. Eur J Radiol 2009;72(1):104-13

21. Koopman D, van Dalen JA, Stevens H, Slump CH, Knollema S, Jager PL. Performance of digital PET compared to high-resolution conventional PET in patients with cancer. J Nucl Med 2020.

22. Nguyen NC, Vercher-Conejero JL, Sattar A, Miller MA, Maniawski PJ, Jordan DW, et al. Image Quality and Diagnostic Performance of a Digital PET Prototype in Patients with Oncologic Diseases: Initial Experience and Comparison with Analog PET J Nucl Med 2015; 56(9):1378-85.

23. Goerres GW, Hany TF, Kamel E, von Schulthess GK, Buck A. Head and neck imaging with PET and PET/CT: artefacts from dental metallic implants. Eur J Nucl Med Mol Imaging 2002;29(3):367-70.

24. Kinahan PE, Hasegawa BH, Beyer T. X-ray-based attenuation correction for

positron emission tomography/computed tomography scanners. Semin Nucl Med 2003;33(3):166-79.

25. Shimamoto H, Kakimoto N, Fujino K, Hamada S, Shimosegawa E, Murakami S, et al. Metallic artifacts caused by dental metal prostheses on PET images: a PET/CT phantom study using different PET/CT scanners. Ann Nucl Med 2009;23(5):443-9.

26. Suzuki A, Ito M, Kawai Y. Dentures wearing reduce motion artifacts related to tongue movement in magnetic resonance imaging. J Prosthodont Res 2018;62(3):303-8.

27. Lwin CT, Hanlon R, Lowe D, Brown JS, Woolgar JA, Triantafyllou A, et al. Accuracy of MRI in prediction of tumour thickness and nodal stage in oral squamous cell carcinoma. Oral Oncol 2012;48(2):149-54.

28. Goel V, Parihar PS, Parihar A, Goel AK, Waghwani K, Gupta R, et al. Accuracy of MRI in Prediction of Tumour Thickness and Nodal Stage in Oral Tongue and Gingivobuccal Cancer With Clinical Correlation and Staging. J Clin Diagn Res 2016;10(6):TC01-5.

29. Iwai H, Kyomoto R, Ha-Kawa SK, Lee S, Yamashita T. Magnetic resonance determination of tumor thickness as predictive factor of cervical metastasis in oral tongue carcinoma. Laryngoscope 2002;112(3):457-61.

30. Preda L, Chiesa F, Calabrese L, Latronico A, Bruschini R, Leon ME, et al.

Relationship between histologic thickness of tongue carcinoma and thickness estimated from preoperative MRI. European radiology 2006;16(10):2242-8.

31. Jung J, Cho NH, Kim J, Choi EC, Lee SY, Byeon HK, et al. Significant invasion depth of early oral tongue cancer originated from the lateral border to predict regional metastases and prognosis. Int J Oral Maxillofac Surg 2009;38(6):653-60.

Figure Legends

Figure 1

T1 tumor cases examined by the SiPM PET (a–c) and non-SiPM PET (d-f). The macroscopic finding shows a T1 tumor in the right (a) or left (d) lateral tongue. Post-contrast T1-weighted image depicts the T1 tumor in both cases (b: major axis 12 mm, thickness 4 mm; d: major axis 17 mm, thickness 4 mm). SiPM PET (c) detected the T1 tumor whereas non-SiPM PET (f) could hardly detect it. SiPM = silicon photomultiplier, SUVmax = maximum standardized uptake value.

Figure 2

T3 tumor cases examined by the SiPM PET (a–c) and non-SiPM PET (d–f). Post-contract T1-weighted image depicts the T3 tumor in both cases (a, b: major axis 31 mm, thickness 17 mm; d, e: major axis 31 mm, thickness 17 mm). SiPM PET (c) and non-SiPM PET (f), both detected the T3 tumors. SiPM = silicon photomultiplier, SUVmax = maximum standardized uptake value.

Figure 3

Detection sensitivity of T1/T2 (a) and T3/T4 (b) primary tumors in SiPM PET and non-

SiPM PET. Mean SUVmax of T1/T2 (c) and T3/T4 (d) primary tumor in SiPM PET and non-SiPM PET. SUVmax = maximum standardized uptake value, SiPM = silicon photomultiplier. N.S. = not significant. Fisher's exact test: †P < 0.05. Welch's *t*-test: ‡P < 0.05.

Figure 4

Correlation between the pathological and the MRI-based or PET-based tumor size. The correlation between the pathological and MRI-based long axis (a), pathological and MRI-based thickness (b), pathological and SiPM PET-based long axis (c), pathological and SiPM PET-based thickness (d), pathological and non-SiPM PET-based long axis (e), and pathological and non-SiPM PET-based thickness (f). SiPM = silicon photomultiplier. N.S. = not significant. Spearman's rank correlation coefficient (ρ) test: *p < 0.05, **p < 0.01, ***p < 0.001

Figure 5

Correlation between the MRI-based and PET-based tumor size in the T1/T2 lesions. The correlation between the MRI-based and SiPM PET-based long axis (a), MRI-based and non-SiPM PET-based long axis (b), MRI-based and SiPM PET-based thickness (c),

MRI-based and non-SiPM PET-based thickness (d), MRI-based and SiPM PET-based volume (e), and MRI-based and non-SiPM PET-based volume (f). SiPM = silicon photomultiplier, N.S. = not significant. Spearman's rank correlation coefficient (ρ) test: **p < 0.01, ***p < 0.001

Figure 6

Correlation between the MRI-based tumor size and SUVmax. The correlation between the MRI-based long axis and SUVmax in the SiPM PET (a), MRI-based long axis and SUVmax in the non-SiPM PET (b), MRI-based thickness and SUVmax in the SiPM PET (c), MRI-based thickness and SUVmax in the non-SiPM PET (d), MRI-based volume and SUVmax in the SiPM PET (e), and MRI-based volume and SUVmax in the non-SiPM PET (f). SUVmax = maximum standardized uptake value, SiPM = silicon photomultiplier. Spearman's rank correlation coefficient (ρ) test: *p < 0.05, **p < 0.01, ***p < 0.001

Acknowledgments

We would like to thank Editage (www.editage.com) for English language editing.

Compliance with ethical standards

Conflict of interest

None of the authors have any conflicts of interest to declare.

Figure 1

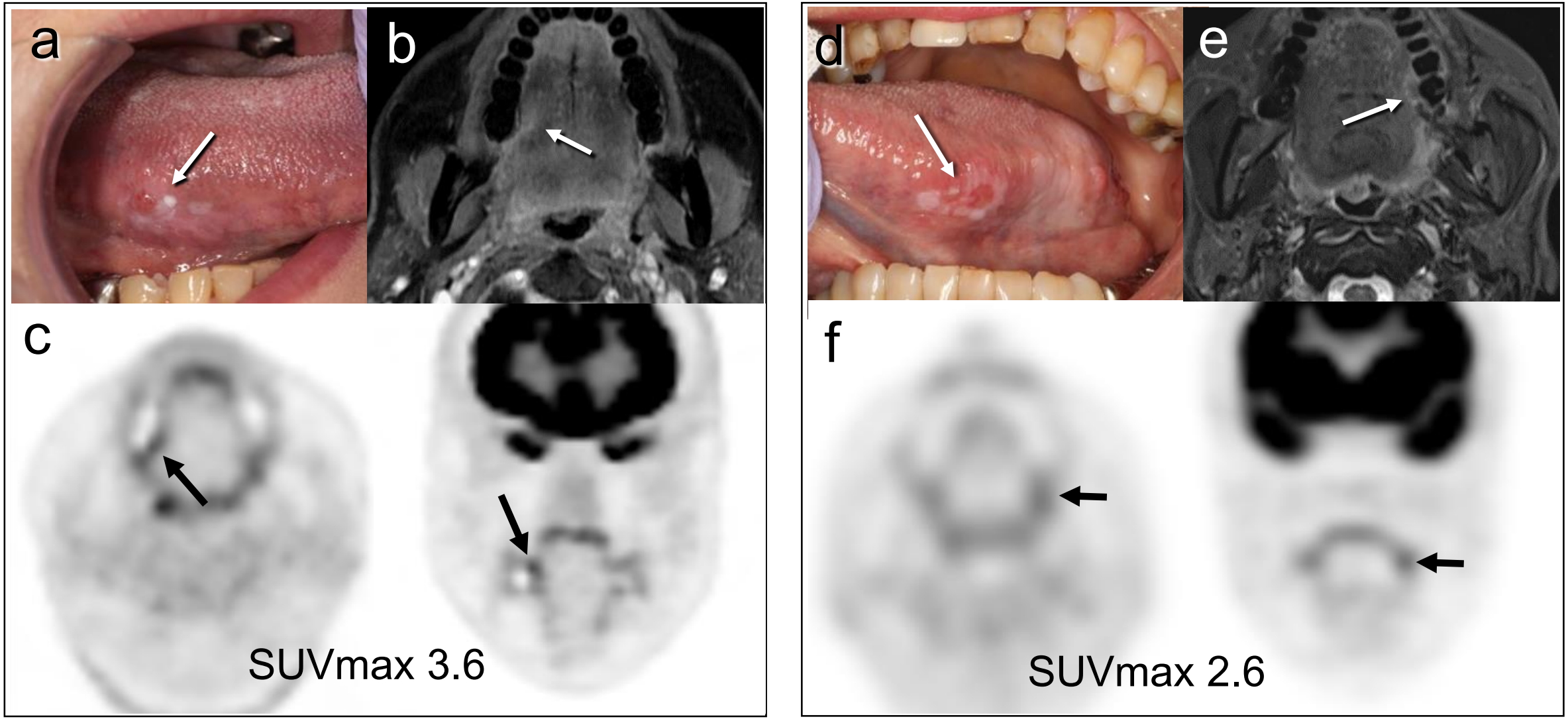

Figure 2

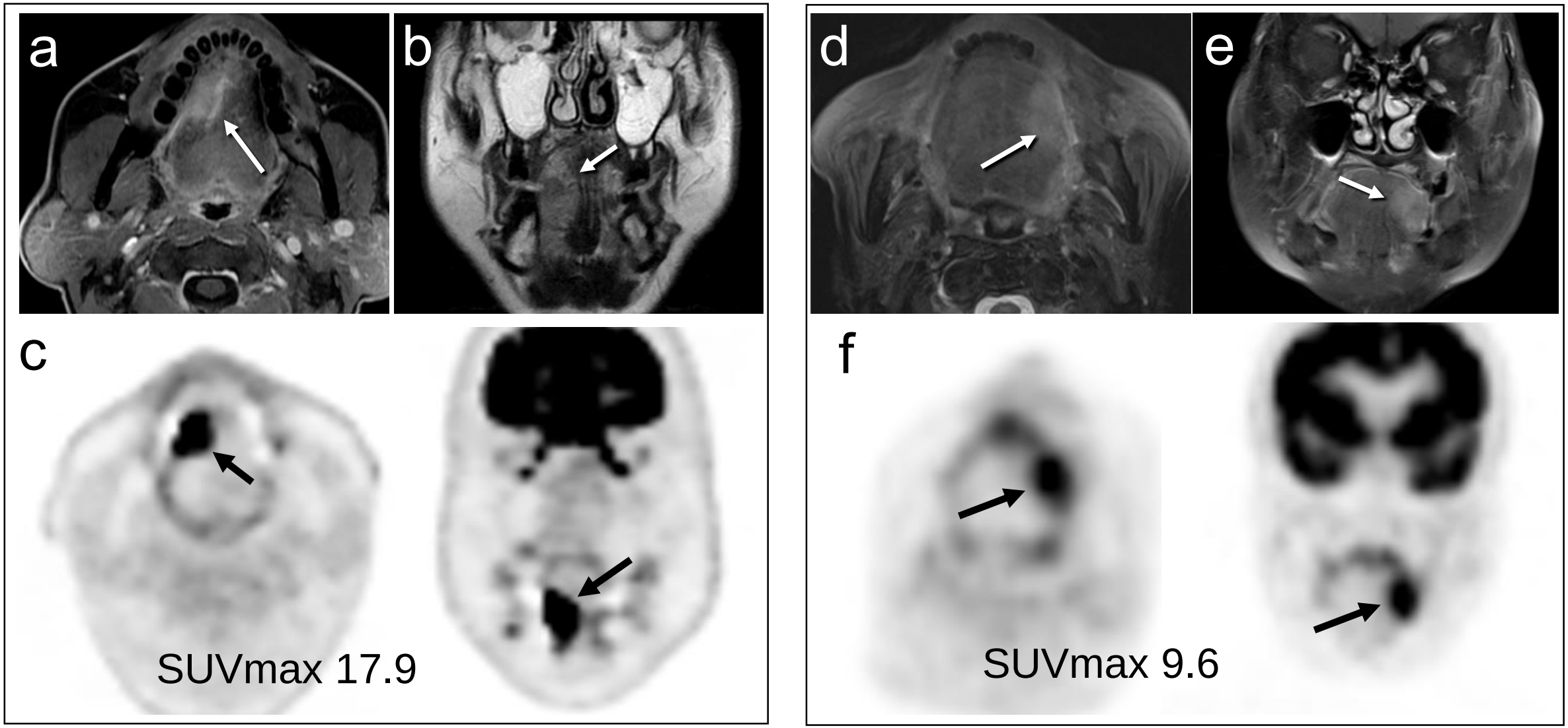

Figure 3

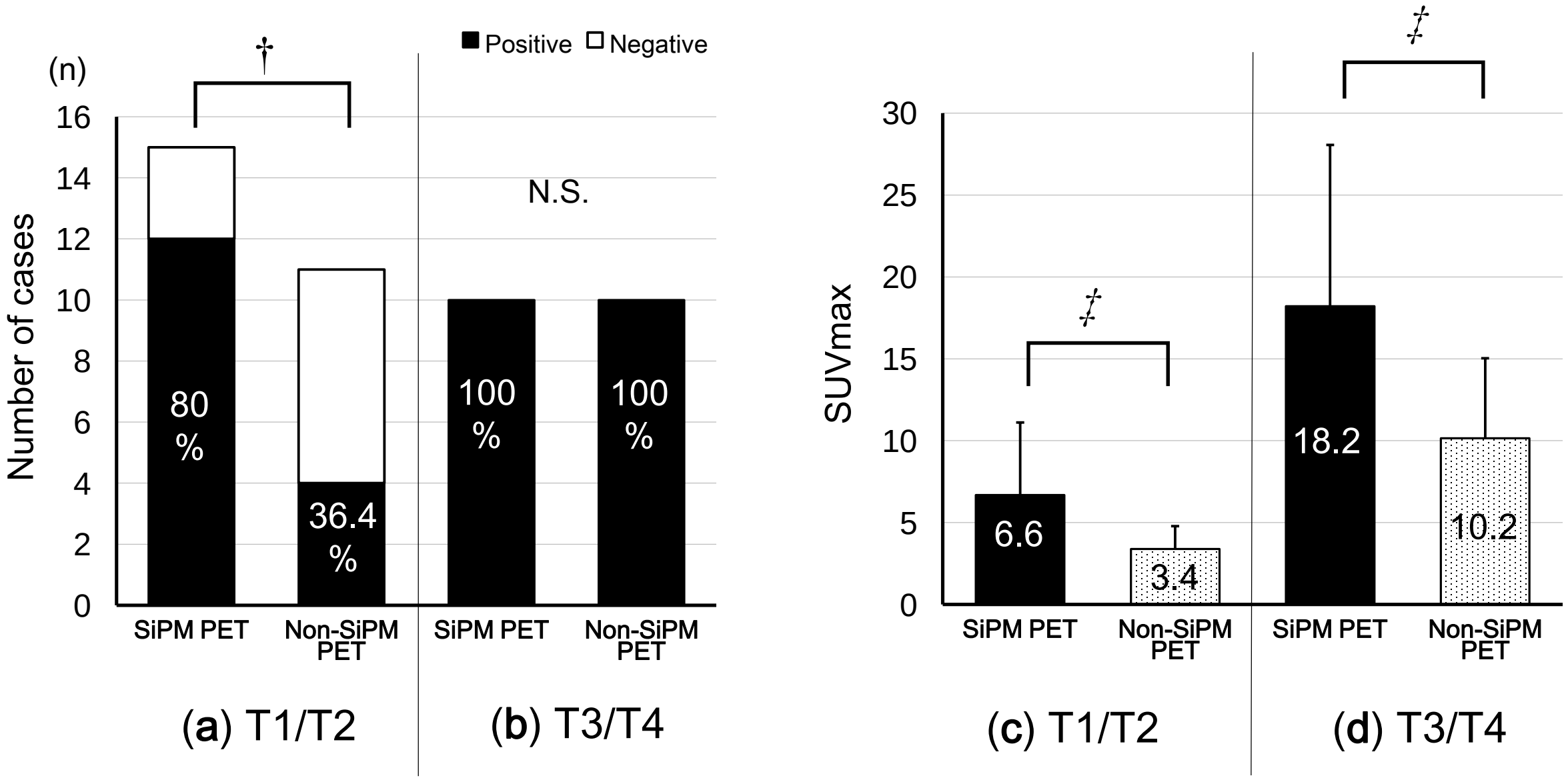
Positive
Negative
(n)
Number of cases
16
14
12
10
8
6
4
2
0
†
80 %
36.4 %
N.S.
100 %
100 %
SiPM PET
Non-SiPM PET
SiPM PET
Non-SiPM PET
(a) T1/T2
(b) T3/T4
SUVmax
30
25
20
15
10
5
0
‡
‡
6.6
3.4
18.2
10.2
SiPM PET
Non-SiPM PET
SiPM PET
Non-SiPM PET
(c) T1/T2
(d) T3/T4

Figure 4

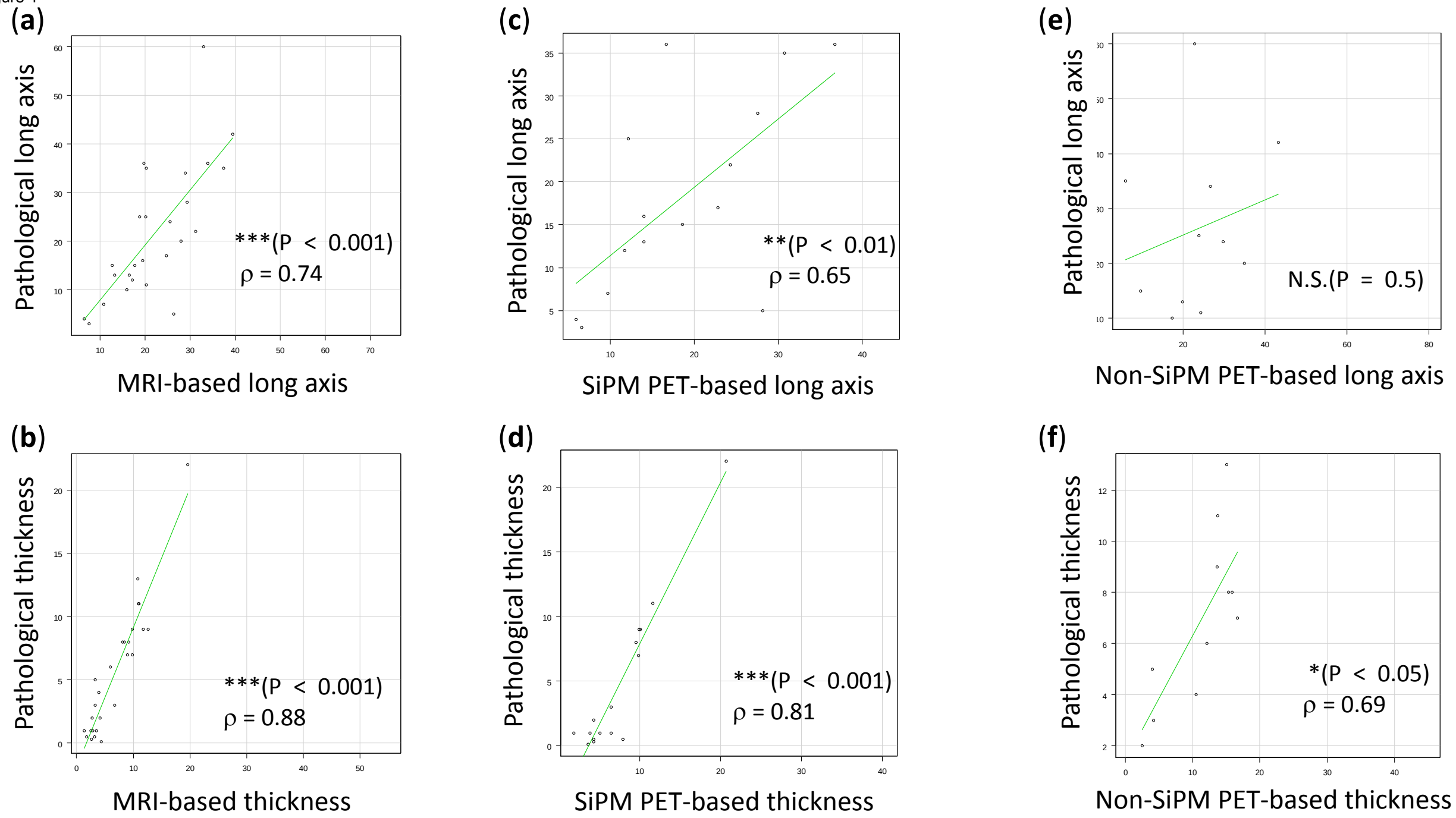
(a)
Pathological long axis
MRI-based long axis
***(P < 0.001)
ρ = 0.74
(c)
Pathological long axis
SiPM PET-based long axis
**(P < 0.01)
ρ = 0.65
(e)
Pathological long axis
Non-SiPM PET-based long axis
N.S.(P = 0.5)
(b)
Pathological thickness
MRI-based thickness
***(P < 0.001)
ρ = 0.88
(d)
Pathological thickness
SiPM PET-based thickness
***(P < 0.001)
ρ = 0.81
(f)
Pathological thickness
Non-SiPM PET-based thickness
*(P < 0.05)
ρ = 0.69

Figure 5

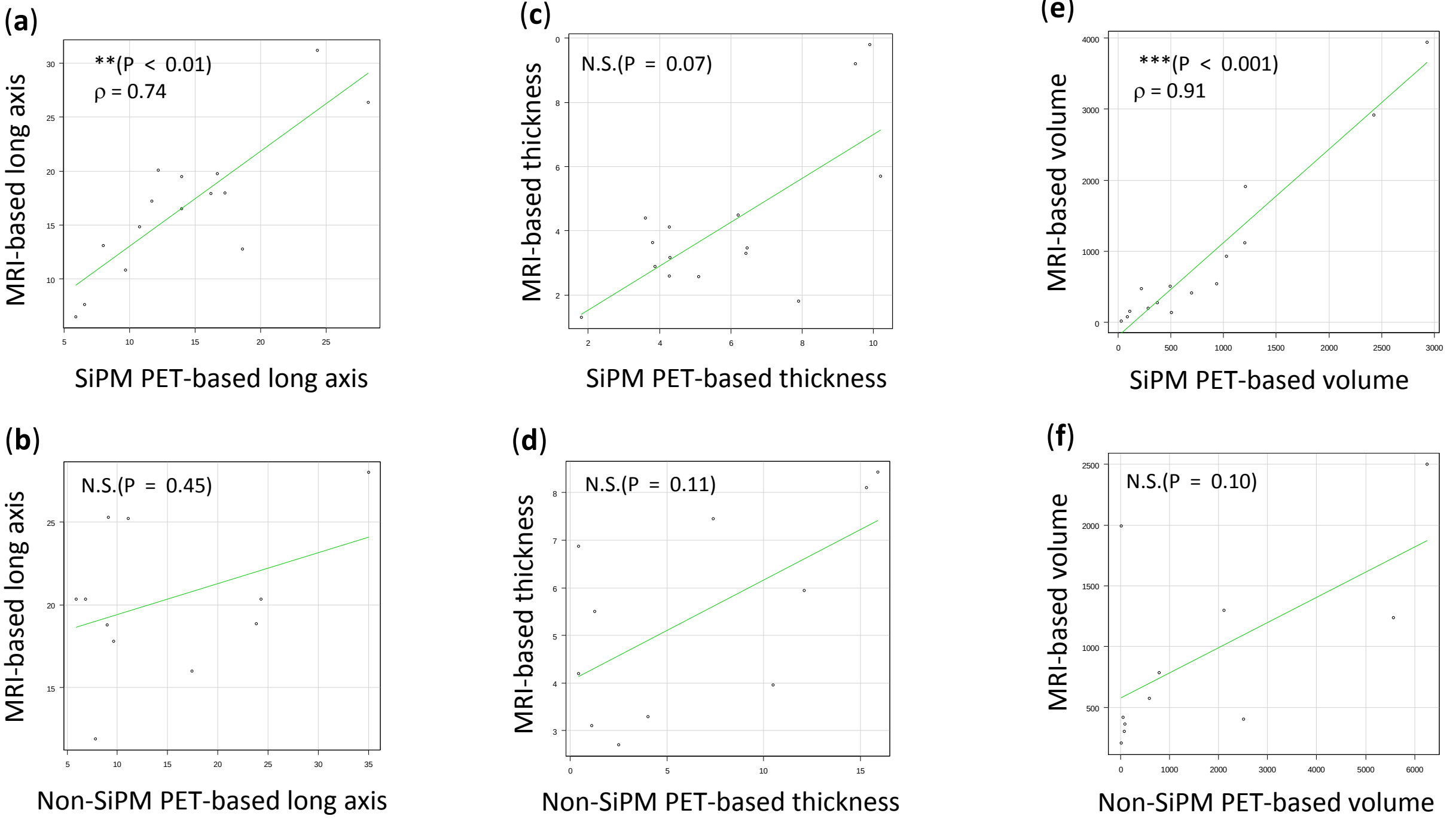
(a)
**(P < 0.01)
ρ = 0.74
MRI-based long axis
SiPM PET-based long axis
(c)
N.S.(P = 0.07)
MRI-based thickness
SiPM PET-based thickness
(e)
***(P < 0.001)
ρ = 0.91
MRI-based volume
SiPM PET-based volume
(b)
N.S.(P = 0.45)
MRI-based long axis
Non-SiPM PET-based long axis
(d)
N.S.(P = 0.11)
MRI-based thickness
Non-SiPM PET-based thickness
(f)
N.S.(P = 0.10)
MRI-based volume
Non-SiPM PET-based volume

Figure 6

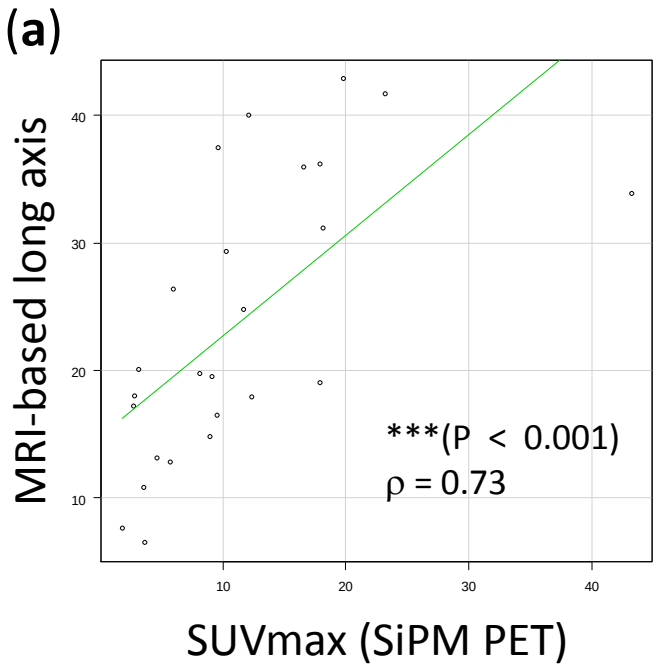
(a)
MRI-based long axis
SUVmax (SiPM PET)
***(P < 0.001)
ρ = 0.73

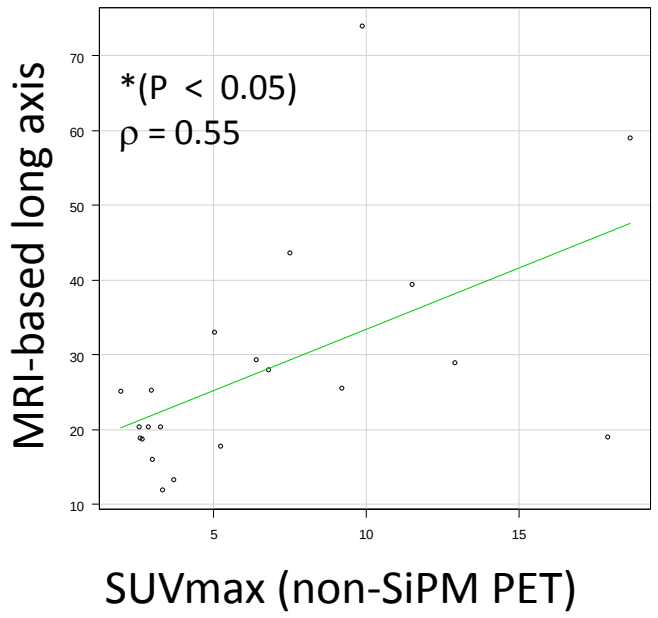
(b)
MRI-based long axis
SUVmax (non-SiPM PET)
*(P < 0.05)
ρ = 0.55

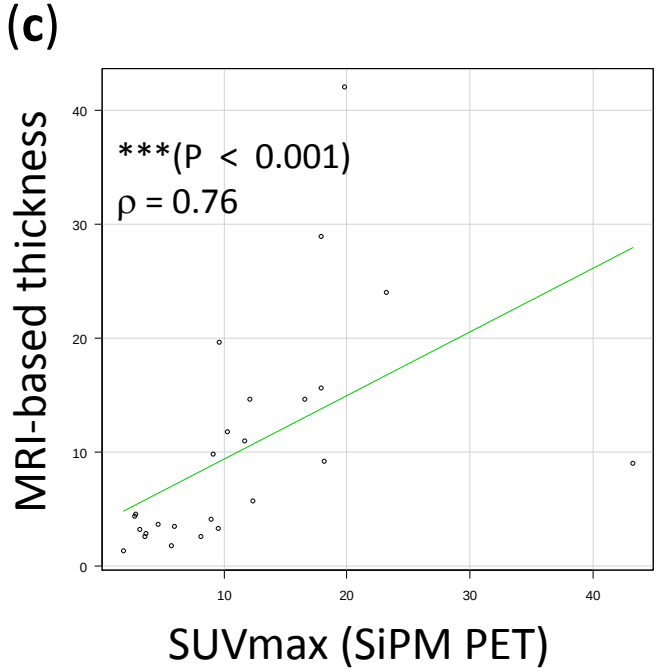
(c)
MRI-based thickness
SUVmax (SiPM PET)
***(P < 0.001)
ρ = 0.76

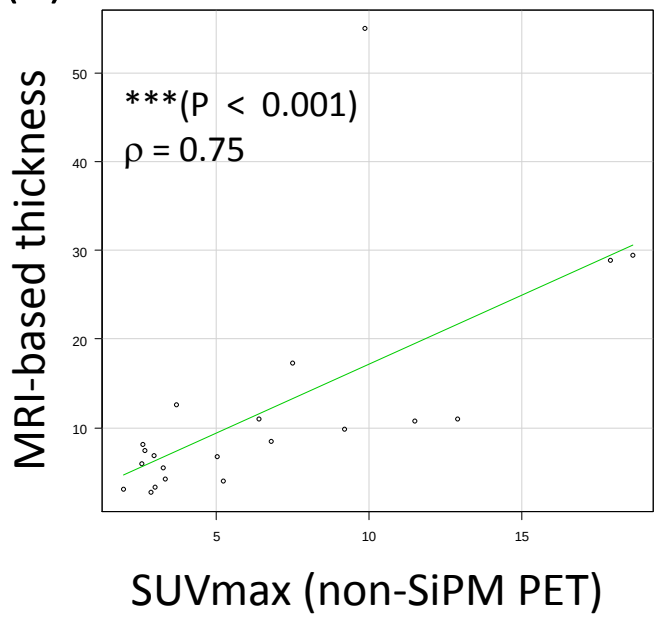
(d)
MRI-based thickness
SUVmax (non-SiPM PET)
***(P < 0.001)
ρ = 0.75

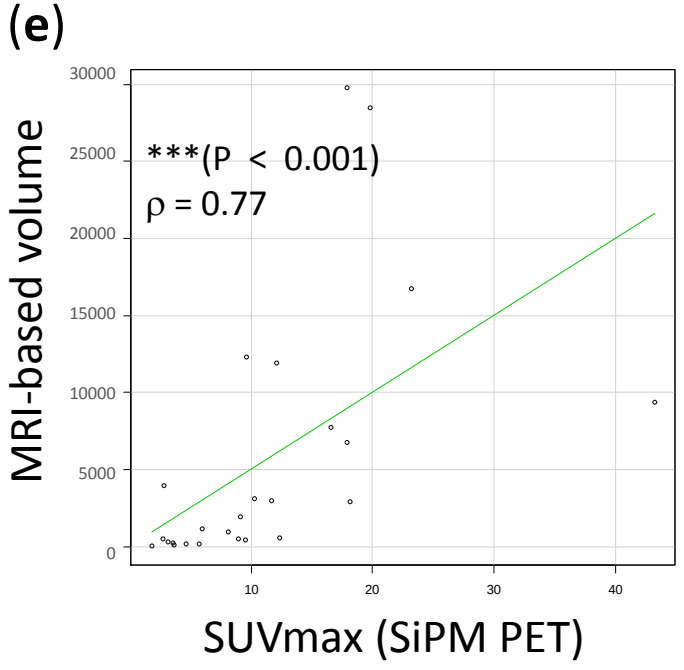
(e)
MRI-based volume
SUVmax (SiPM PET)
***(P < 0.001)
ρ = 0.77

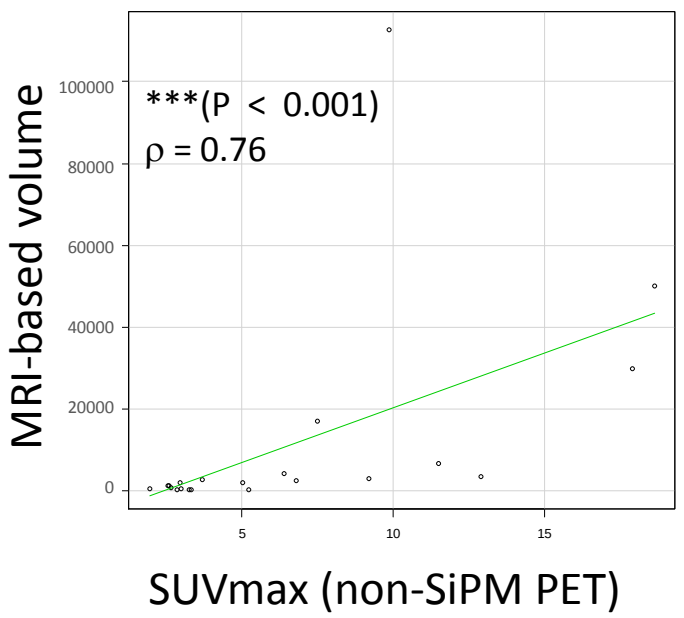
(f)
MRI-based volume
SUVmax (non-SiPM PET)
***(P < 0.001)
ρ = 0.76

Table 1. Clinical Characteristics of Study Population

		SiPM PET	non–SiPM PET	
Characteristics of patients	Number of patients	25	21	
	Male:Female	12:13	14:7	†N.S.
	Mean age (years)	66.1 ± 19.4	65.6 ± 10	‡N.S.
T category	T1	6	3	†N.S.
	T2	9	8	
	T3	6	5	
	T4	4	5	
T1/T2 morphology	Major axis (mm)	17.2 [13.0–19.6]	20.3 [18.3–22.8]	#N.S.
	Thickness (mm)	3.5 [2.7–4.4]	5.5 [3.6–7.2]	#N.S.
	Volume (cm^3)	0.48 [0.18–1.02]	0.57 [0.38–1.27]	#N.S.
T1/T2 histopathology	Mode of invasion	3 [2–3]	3 [2–3]	#N.S.
	Degree of differentiation	1 [1–1]	1 [1–1]	#N.S.
T3/T4 morphology	Major axis (mm)	36.1 [30.5–39.3]	31.2 [26.4–42.7]	#N.S.
	Thickness (mm)	15.1 [12.5–22.9]	11.8 [10.9–26.0]	#N.S.
	Volume (cm^3)	10.6 [7.0–15.6]	5.41 [3.14–26.6]	#N.S.
T3/T4 histopathology	Mode of invasion	2 [2–3]	3 [3–3.25]	#N.S.
	Degree of differentiation	1 [1–1]	1 [1–1]	#N.S.

SiPM = silicon photomultiplier. Mode of invasion: modified Jakobsson criteria, Degree of differentiation: WHO classification of tumor malignancy gradation. †Fisher's exact test, ‡Welch's *t*-test, #Mann–Whitney U test, N.S.: not significant. Data are presented as mean ± standard deviation, median [interquartile rage] or number, as appropriate.